1B17

HORIZONTAL FLOW STRUCTURE IN CHANNELS WITH DENSE VEGETATION CLUSTERS AND THE NUMERICAL ANALYSIS THEREOF

SHOJI FUKUOKA
Professor, Hiroshima University, Higashi-Hiroshima, 724, Japan
AKIHIDE WATANABE
Senior Research Engineer, Public Works Research Institute,
Ministry of Construction, Tukuba, Ibaragi, 305, Japan

ABSTRACT

This paper, focusing on horizontal large-scale eddies in channels with dense vegetation clusters and on the regular surface fluctuation that occurs downstream as a result, explains the structure of horizontal flow conditions using analysis based on laboratory experiments and a shallow-water equation devised with a model of horizontal mixing. The results of numerical analysis of horizontal velocity fields, water surface fluctuation fields and predominant wavelengths -- determined through shallow water equation -- accurately correspond to experimental results and enable predictions of sufficient accuracy.

1. INTRODUCTION

Velocity in rivers of dense vegetation clusters is extremely low, resulting in large differences in velocity with the main current. This, in turn, results in vigorous momentum exchange between the flow in vegetation clusters and the main current and in horizontal mixing with a large transverse water-level gradient around the vegetation. Mixing with this type of horizontal large-scale eddies becomes a resistance factor of the flow. [1)2)3)]

In this research, we performed a hydraulic model experiment on a flow field with typical patterns of vegetation growth in order to determine the characteristics of the flow field. Next, we developed a simple, two-dimensional (horizontal) model of horizontal mixing that is caused by vegetation, then used this model to determine the predominant wavelength as a nonlinear stability problem. Finally, we investigated the structure of horizontal mixing and horizontal flow conditions by solving this model and comparing these results with those of our experiments.

2. EXPERIMENT ON HORIZONTAL MIXING CAUSED BY VEGETATION CLUSTERS

(1) EXPERIMENTAL PROCEDURE

For our cases of rivers with conspicuous horizontal mixing caused by vegetation clusters, we performed channel experiments with uniform, continuous vegetation growing in the center of the channel and uniform, continuous vegetation growing along the banks of the main channel in a course with a compound section.

The channel used in these experiments was a straight channel, made of steel, with a uniform rectangular section, 15m in length, 1.2m in width, and a bed slope of 1/1000. The Manning roughness coefficient of the channel bottom is 0.011. The experiment in which vegetation was placed in the center of the channel is named "Case A". In "Case B", a flood channel was created by affixing pieces of plywood 40cm wide and 2cm high along the length of the channel to perform an experiment on a compound section channel with a ratio of main channel width to flood channel height of 20 and a ratio of main channel width to total width of 1/3. The flood channel was covered with geotextile sheet in order to give it a higher roughness coefficient than the main channel. A porous vegetation

HYDRA 2000 (Vol. 1). Thomas Telford, London, 1995

model made of plastic (91% porosity, permeability coefficient K = 0.38m/s) was used.

(2) RESULTS OF EXPERIMENT ON CASE A

Velocity and water level fluctuation were measured under the following conditions: vegetation cluster width b' = 10cm; vegetation height h = 4cm; discharge Q = 11 l/s (flow depth h = 4.5cm).

Figure 1 shows velocity fluctuations u' and v' and water level fluctuation η' measured near the vegetation cluster. Velocity and depth were measured respectively with a two-component electromagnetic current meter and a capacitance-type wave gage, which were attached opposite from each other next to the vegetation cluster. Both velocity and water level fluctuated nearly periodically, with the phases of u' and v' diverging by one-half period. Consequently, Reynolds stress also fluctuated periodically, showing a large peak value. The fact that the phases of η' and v' nearly coincide near the vegetation and that the phases of η' on either side of the vegetation cluster are reversed[2)3)] shows that a flow from higher to lower areas in the water surface is being produced on either side of the vegetation cluster.

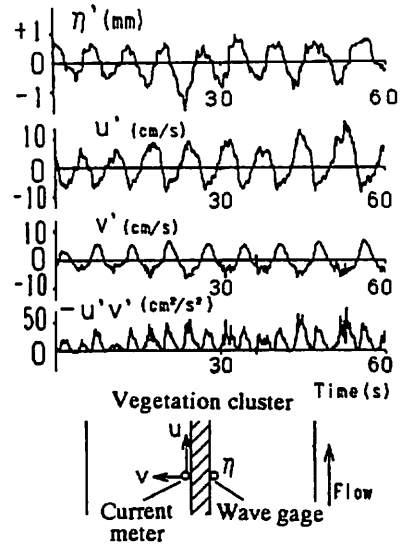

Fig. 1 Changes over time in water level and velocity near the vegetation cluster

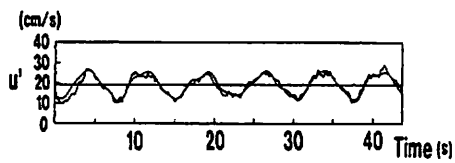

(a) Changes over time in u'

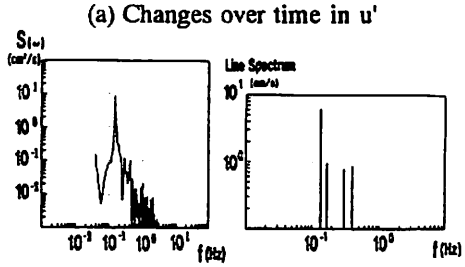

(b) Power spectrum density (c) Line spectrum

Fig. 2 Spectrums of velocity fluctuation u'

Figure 2 shows power spectrum density $S(\omega)$ at various frequencies ω for the waveforms of velocity fluctuation u' as measured at a position 15 cm from the vegetation boundary towards the main current. (Line spectrums are also shown.) In Figure 2 the waveforms are represented with measured values (thin line) and the dominant fluctuation component of line spectrum (thick line). $S(\omega)$ has a large low-frequency range and a clear peak, while the frequency indicated by the line spectrum diagram generally complies with the measured waveform. Figure 3 shows a contour of surface level; high and low parts in the surface regularly appear in the longitudinal direction, and that the two sides separated by the vegetation have crests and troughs in the surface that have laterally opposite phases. We see that horizontal eddies occur in depressed parts of the surface; more specifically, that horizontal large-scale eddies appear alternately on the left and right sides of the vegetation cluster and maintain this configuration as they move downstream.

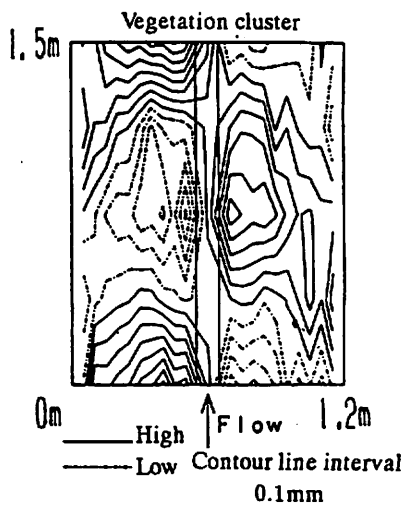

Fig. 3 Surface level contour

(3) RESULTS OF EXPERIMENT ON CASE B

As in Case A, in Case B water surface profile, velocity fluctuation and other factors were measured and displayed visibly under conditions at which mixing is the most prominent. With a constant vegetation width b' of 3.5cm, measurements were performed with a continuous configuration (height, 6.5cm). Figure 4, a contour of surface level measured with a discharge of 9 l/s (depth h = 6.8cm) shows that crests and troughs in the surface appear alternately in the downstream direction in the main channel. In Photo 1 aluminum powder was used to make the horizontal flow

conditions visible: aluminum powder meanders through the main channel, while lines of aluminum powder can also been seen in the flood channel. Figure 5, a graphic representation based on Figure 4 and Photo 1, shows that in areas of low water level in the main channel there are horizontal eddies around which the aluminum powder is concentrated. It is likely that the aluminum powder meanders because of these eddies, which proceed, alternately left then right, down the main channel. With the horizontal eddies that form in the flood channel revolving in the opposite direction of those in the main channel, these eddies, alternately revolving in opposite directions, cause the characteristic whiskerlike lines to appear at Location A, the position in the flood channel where the flow concentrates. In this case, the phases of these whiskerlike lines on the left and right sides are out of synchronization by π.

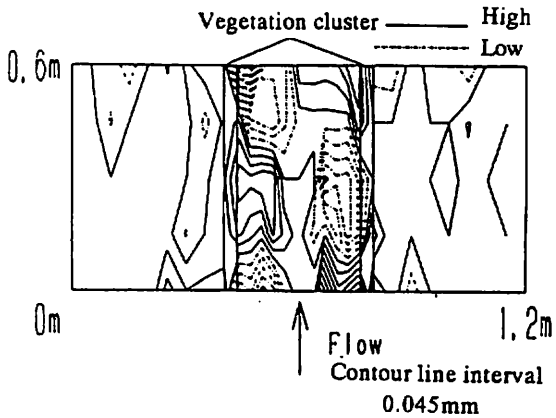

Fig. 4 Contour of water level (case B)

Photo 1: Photo of Case B

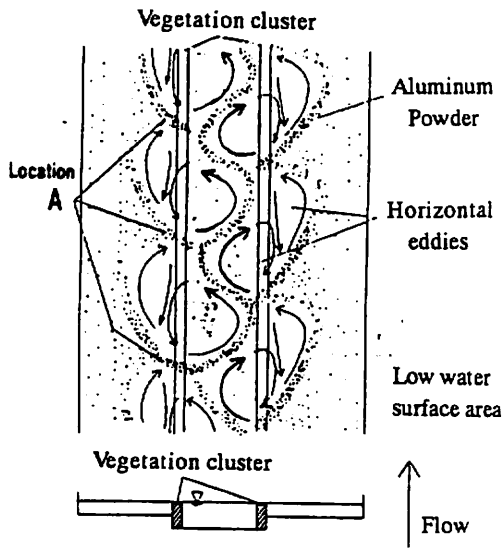

Fig. 5 Illustration of Case B

3. NUMERICAL ANALYSIS OF HORIZONTAL FLOW FIELD

(1) METHOD OF ANALYSIS

The basic equations for flows where vegetation is present is represented with (1), (2), and (3).

$$\frac{\partial u}{\partial t}+u\frac{\partial u}{\partial x}+v\frac{\partial u}{\partial y}=gI-g\frac{\partial \eta}{\partial x}-\frac{c_f u\sqrt{u^2+v^2}}{h_o}-g\frac{u\sqrt{u^2+v^2}}{k^2}+\nu_t\left\{\frac{\partial}{\partial x}\left(2\frac{\partial u}{\partial x}\right)+\frac{\partial}{\partial y}\left(\frac{\partial u}{\partial y}+\frac{\partial v}{\partial x}\right)\right\} \quad (1)$$

$$\frac{\partial v}{\partial t}+u\frac{\partial v}{\partial x}+v\frac{\partial v}{\partial y}=-g\frac{\partial \eta}{\partial y}-\frac{c_f v\sqrt{u^2+v^2}}{h_o}-g\frac{v\sqrt{u^2+v^2}}{k^2}+\nu_t\left\{\frac{\partial}{\partial x}\left(\frac{\partial v}{\partial x}+\frac{\partial u}{\partial y}\right)+\frac{\partial}{\partial y}\left(2\frac{\partial v}{\partial y}\right)\right\} \quad (2)$$

$$\frac{\partial \eta}{\partial t}+\frac{\partial(\eta u)}{\partial x}+\frac{\partial(\eta v)}{\partial y}=0 \quad (3)$$

The following equation was used for the eddy viscosity coefficient (υ_t).

$$\nu_t=\frac{1}{6}\kappa u_* h_o \quad (4)$$

where u is the depth-averaged velocity in the downstream direction; v, the depth-averaged velocity in the transverse direction; η, depth; g, gravitational acceleration; c_f, friction resistance coefficient; κ, von Karman's constant (0.4); u_*, friction velocity; h_o, average depth. K, permeability coefficient, represents the permeation of the vegetation. U_w, the apparent velocity inside the vegetation cluster, is represented with permeability coefficient K and energy gradient Ie as shown in equation (5)[2)3)].

$$U_w=KI_e^{1/2} \quad (5)$$

Next, we shall discuss the development of a model for horizontal mixing. Velocities u and v and water depth η are divided into their average values and the amount of fluctuation therefrom.

Fluctuation quantities are represented by superimposing the first-order mode of wavelength L and the second-order mode of wavelength L/2.

$$u(x,y,t,)=u_0(y,t)+\sum_{m=1}^{2} u_m(y,t)\cos\frac{2m\pi}{L}(x-ct+\alpha_m(y)) \quad (6)$$

$$v(x,y,t,)=v_0(y,t)+\sum_{m=1}^{2} v_m(y,t)\cos\frac{2m\pi}{L}(x-ct+\beta_m(y)) \quad (7)$$

$$\eta(x,y,t,)=h_0(y,t)+\sum_{m=1}^{2} \eta_m(y,t)\cos\frac{2m\pi}{L}(x-ct+\gamma_m(y)) \quad (8)$$

The reason for incorporating the secondary mode into fluctuations is because of the mixing phenomenon is determined by mixing of a scale corresponding to that of large-scale horizontal mixing.

Substituting u, v, and η in equations (6), (7), and (8) into basic equations (1), (2), and (3) produces 15 simultaneous partial differential equations for unknown variables$_1$, u_o v_o, and h_o ; fluctuation amplitudes u_1, u_2, v_1, v_2, η_1, and η_2; and phase differences $\gamma_1 - \alpha_1$, $\gamma_1 - \alpha_2$, $\gamma_1 - \beta_2$, $\gamma_1 - \gamma_2$ and wave speed c. An arbitrary value is given to γ_1. The solution is obtained by assigning the small disturbance of 1/100 of measured depth to an initial water level and then time-integrating these unsteady terms explicitly. The restrictive condition assigned is a discharge-constant condition. In this model, the predominant fluctuation components of u, v, and η are extracted and a wave-motion shape is assigned for the downstream direction in order to make this a one-dimensional problem for the transverse direction.

(2) CALCULATING THE PREDOMINANT WAVE NUMBER AS A NONLINEAR STABILITY PROBLEM

We will first determine, through numerical analysis, the predominant wave number of a periodic eddy. Ikeda et al[5]. have performed a linear stability analysis on periodic eddies that form near vegetation boundaries, and have attempted to determined the predominant wave number of small disturbance in a flow with an assigned velocity distribution. However, because wave number and velocity distribution are interrelated, they should be determined simultaneously as a nonlinear relationship.

The analytic method described in section 3.(1) was used to determine the predominant wave number through nonlinear stability analysis in which velocity distribution is calculated with different wave numbers. The occurrence of predominant wave number is assumed when the value of Reynolds stress due to large-scale eddy near the vegetation boundary is maximum with respect to wave number.

To determine this, we calculated the maximum value of Reynolds stress at various wave numbers using the experimental values of Fukuoka and Fujita[2)3)] and the authors' experimental values. The conditions used in calculations by Fukuoka et al. are in Table 1 and the results of these calculations are in Figure 6. Reynolds stress for the velocity field of the first-order mode has a peak at wave number k, indicating the existence of a wave number region where horizontal mixing is most vigorous. However, it appears that this peak wave number has a certain width. The time required for Reynolds stress to achieve a stabilized value after the beginning of progression is expressed in the diagram as Tg. It can be seen that the higher the frequency is, the shorter the time required for stabilization is.

In other words, in the group of wave numbers at which Reynolds stress peaks, those with higher frequencies progress faster. It is possible that a stable field is formed at the stage at which this eddy fully progresses, after which eddies with smaller wave numbers can no long progress. In actual experiments performed by Fukuoka and Fujita with a 50-m-long channel, a wavelength of 3.5m was observed, and was situated in the region with the largest wave number in this gentle peak.

Similarly, predominant wave number of calculation for Case B agree well with the result of experiment as shown in Figure 7.

Table 1 : Experimental conditions used in calculations[2)3)]

Discharge (l/s)	Bed slope	Uniform depth(cm)	channel width (cm)	Vegetation width (cm)	Bed roughness	Permeability coefficient(m/s)
37	1/1000	4.5	300	30	0.011	0.38

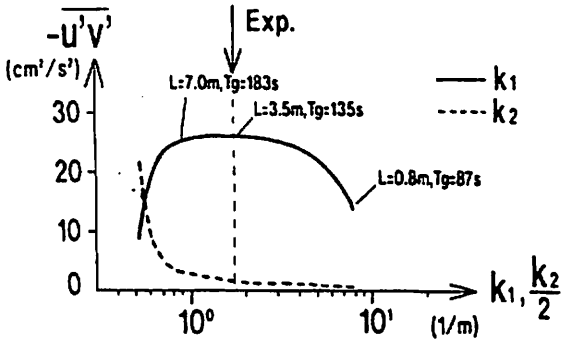

Fig. 6 Relationship between Reynolds stress and wave number, (Fukuoka and Fujita)

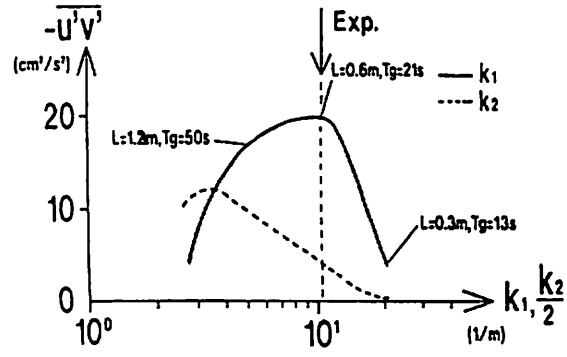

Fig. 7 Relationship between Reynolds stress and wave number (Case B)

(3) RESULTS OF CALCULATIONS FOR CASE B

Here, we shall present the results for the stage in which the flow has developed sufficiently. Figures 8 and 9 respectively show the velocity vector in a stationary coordinate system, and the contour of the surface. They show that laterally alternate large-scale horizontal eddies have formed in the main channel, and that the surface is lower in these areas. The flow meanders along the periphery of these horizontal eddies in the main channel, accurately corresponding with the experimental results shown in Fig. 4 and Photo 1. The periphery of these eddies passes through the vegetation into the flood channel. Figures 10 and 11 respectively show the depth-averaged velocity distribution and Reynolds stress distribution. The calculated and measured values for depth-average velocity distribution generally correspond. The fact that the velocity in the main channel is roughly the same as in the flood channel in spite of the lower roughness coefficient and shallower depth in the main channel indicates that in the main channel, velocity is being reduced by horizontal mixing. The distribution of Reynolds stress has a larger peak value on the main channel side. This indicates that in a compound channel, horizontal mixing in the main channel predominates.

Next, we visibly represented the calculated flow in order to compare it with the distribution in Photo 1. Here, we examined the movement of markers released downstream into the obtained velocity field. These results are shown in Figure 12.

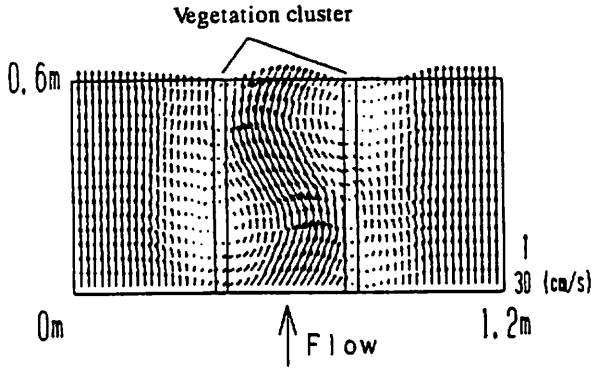

Fig. 8 Calculated velocity vector (Case B)

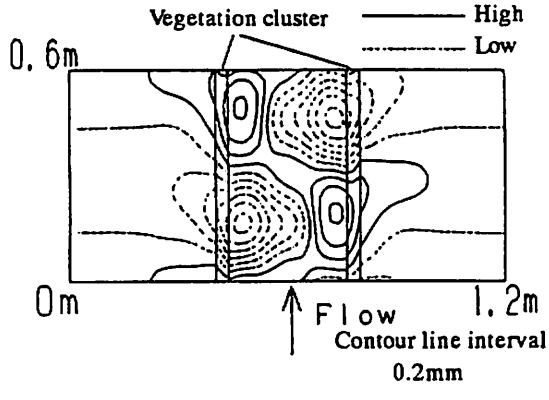

Fig. 9 Calculated water level contour (Case B)

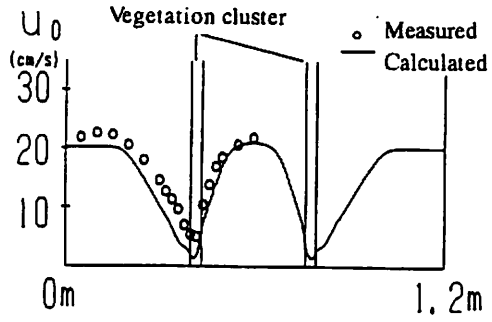

Fig. 10 Depth-averaged velocity distribution (Case B)

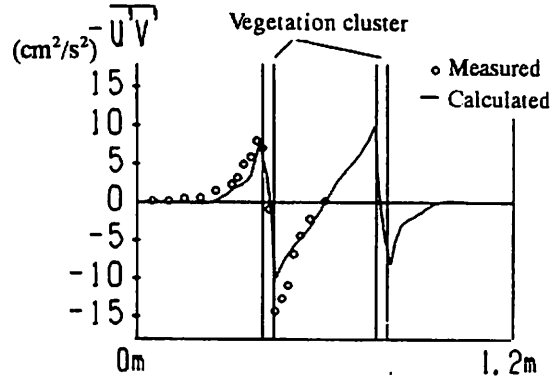

Fig. 11 Reynolds stress distribution (Case B)

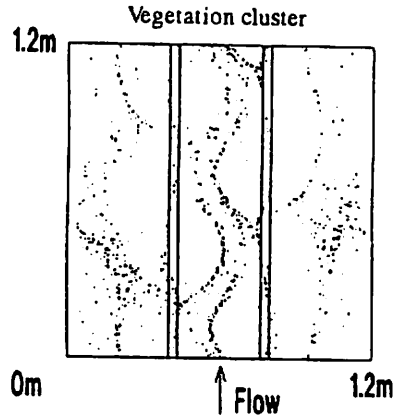

Fig. 12 Marker distribution by calculation (Case B)

As in Photo 1, the markers show a meandering path in the main channel and take on the characteristic whiskerlike lines near the shoulders of the flood channel. As in the experiment, these lines indicate a laterally alternating configuration of horizontal eddies in the main channel, with a resultant π shift in the right and left phases.

4. CONCLUSION

The primary conclusions of this research are as follows.

1. Large-scale horizontal eddies occur near longitudinally continuous vegetation, and their downstream progression causes periodic fluctuation in the surface. Because this eddy formation alternates in the downstream direction between the two sides separated by vegetation, a large surface gradient forms in the transverse direction inside the vegetation cluster. These horizontal eddies and transverse surface gradient cause fluid mixing in the transverse direction.
2. We developed a model of horizontal mixing caused by the presence of vegetation and incorporated it into the basic equations in order to perform nonlinear stability analysis on the flow field. These results showed that it is possible to estimate the predominant wavelength of horizontal eddies.
3. Upon analyzing the flow conditions, horizontal flow conditions and shearing force at the vegetation boundary agreed with the values obtained in experiments to a significant degree, thus demonstrating that such horizontal mixing is determined by predominant wavelengths, such as large-scale horizontal eddies, and that two-dimensional horizontal flow analysis is capable of arriving sufficient solutions.

REFERENCE

1) Fukuoka, S. and Fujita, K. : Water level prediction in river courses with vegetation,'Proc. 25th IAHR Congress, Vol. 1, pp. 177-184, 1993.
2) Fukuoka, S. and Fujita, K. : Hydraulic effects of luxuriant vegetation on flood flow, Report of Public Works Research Institute, Ministry of construction, Vol. 180, pp.1-64, 1990.(in Japanese).
3) Fukuoka, S. and Fujita, K. : Flow resistance due to lateral momentum transport across vegetation in the river course, Int. Conf. on Physical Modeling of Transport and Dispersion, 12B, Boston, pp. 25-30, 1990.
4) Fukuoka,S. Watanabe, A. and Tsumori, T.: Structure of plane shear flow in river with vegetations, J. of Hydraulic, Coastal and Environmental Engineering, JSCE, No.491, pp.41-50, 1994. (in Japanese).
5) Ikeda, S. Ohta, K. and Hasegawa, H. : Periodic vortices at the boundary of vegetated area along river bank, Proc.of Hydraulics and Sanitary Engineering, JSCE, No.443, pp.47-54, 1992. (in Japanese).